Physica E 44 (2012) 2072–2077

Contents lists available at SciVerse ScienceDirect

Physica E

journal homepage: www.elsevier.com/locate/physe

Biosensing potential of three-layered gold–dielectric–gold nanoshells: sensitivity of interdistance of resonance light scattering peaks to the local dielectric environment

Guojun Weng, Jianjun Li, Junwu Zhao*

The Key Laboratory of Biomedical Information Engineering of Ministry of Education, School of Life Science and Technology, Xi'an Jiaotong University, No. 28 Xianning West Road, Xi'an 710049, China

HIGHLIGHTS

- ▸ Three-layered nanoshell has three types of resonance light scattering mode.
- ▸ Enhanced inter-distance shows the ability of three-layered nanoshell in biosensing.
- ▸ Three-layered nanoshell is superior to two-layered nanoshell in RLS detection.
- ▸ Three-layered nanoshell with thick middle shell has the highest sensitivity.

GRAPHICAL ABSTRACT

The physical environment dependent interdistance enhancing between the two peaks shows the potential of the three-layered gold–dielectric–gold nanoshells used in sensing based on RLS.

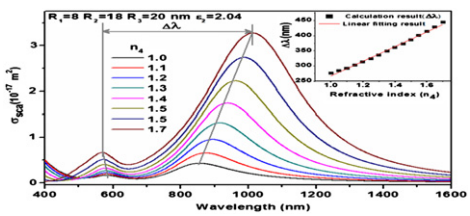

ARTICLE INFO

Article history:
Received 11 November 2011
Received in revised form
1 June 2012
Accepted 22 June 2012
Available online 2 July 2012

ABSTRACT

The resonance light scattering cross section of the three-layered gold–dielectric–gold nanoshell is calculated using the quasi-static theory. The results show that three-layered gold–dielectric–gold nanoshells have three types of resonance light scattering spectra under different geometrical parameters, which are explained using plasmon hybridization theory. In the common type containing two resonance light scattering peaks, the longer wavelength peak red-shifts while the shorter one blue-shifts as the refractive index of the physical environment increase. This physical environment dependent interdistance enhancing between the two peaks shows the potential of the three-layered gold–dielectric–gold nanoshells used as biosensor based on resonance light scattering. The followed calculations about the comparison of sensitivity to the local dielectric environment between the three- and two-layered gold nanoshells further verify that point. At last, the calculated results that the three-layered gold–dielectric–gold nanoshells with small inner core and thin outer gold shell have the highest sensitivity are also obtained.

1. Introduction

Gold nanoparticles and their related nanostructures have fascinated scientists due to their special optical properties [1,2], which are known as surface plasmon resonance (SPR), defined as the collective oscillations of conduction electrons [3]. The frequency of this resonance oscillation can be varied over a wide range by changing size, shape, dielectric surrounding, and composition of the nanoparticles [4,5]. Among these gold related nanostructures, gold nanoshells of two-layered [6–9], three-layered [10–15] and four-layered (concentric double) [16–18], have received particularly significant research attentions.

Typical two-layered gold nanoshells, consisting of a dielectric core surrounded by a thin shell of gold [19], are tunable plasmonic

* Corresponding author. Tel./fax: +86 29 82665626.
E-mail address: nanoptzhao@163.com (J. Zhao).

1386-9477/$ - see front matter © 2012 Elsevier B.V. All rights reserved.
http://dx.doi.org/10.1016/j.physe.2012.06.015

nanostructures, whose plasmon resonance is sensitive to the ratio of the inner core radius to the outer shell radius [18]. With a decrease in the thickness of the gold shell, the plasmon resonance frequency shifts from the visible region towards the near-infrared region [20], where biological tissue has the minimal absorption [21]. This near-infrared property in company with excellent biocompatibility [22], makes gold nanoshell a convenient probe having wide applications [23], such as biomedical imaging [24], bioassay [25], and detecting the changes in dielectric environment [26]. However, the advisable near-infrared property in two-layered gold nanoshells often accompanies with a large nanoshell radius and a thin gold layer [12], which is difficult to achieve [10], and use in tissue penetration.

Recently, three-layered gold–silica–gold nanoshells with a size sub-100 nm have been synthesized by Xia et al. [27]. Wu and Liu [12], and Hu et al. [10], have proved that the extra gold core in three-layered gold–silica–gold nanoshells can turn the near-infrared property and meet the defects of two-layered gold nanoshells. In addition, the inserted gold nanosphere has great effect on the local electric field enhancement at different interfaces and locations of three-layered gold–silica–gold nanoshells [28]. The influence of geometric condition and surrounding medium on the optical properties especially the SPR of three-layered gold–silica–gold nanoshells have been theoretically investigated in detail [10,12,29]. Furthermore, relative absorption and scattering efficiencies of sub-100 nm size three-layered gold–silica–gold nanoshells have been studied, and a third SPR peak which has higher energy was thought as too weak to be observed [30]. However, in the work of Zhu et al. [31], the third SPR peak has been observed and the conditions on which it would occur were given too. The above experimental synthesis and theoretical SPR predicting about three-layered gold–silica–gold nanoshells pave the road for the development of various optical applications using three-layered gold nanoshell.

However, after analyzing the data of Hu et al. [10], we found that the sensitivity of the both SPR peaks of a three-layered gold nanoshell to changes in dielectric environment is lower than a two-layered gold nanoshell with equal overall size and thickness of the outer gold shell. It suggests that a three-layered gold nanoshell would hold gloomy prospects in the sensing applications based on analyzing SPR behaviors. In addition, when involving the SPR detections harnessing gold nanoshells, scientists just pay close attention to the changing of one peak, such as the positions [26], intensity [25], and linewidth [8]. Taking the changes of two or more peaks as a whole is frequently neglected by researchers.

Resonance light scattering (RLS), occurring when the wavelength of the incident light is close to that of the absorption band of the molecular particles [32,33], are better to conventional optical methods for biomedical detection and labeling in several aspects, such as light intensity. For biomedical detections, Shang et al. [34] have developed an enhanced RLS assay for glucose based on biocatalytic growth of gold nanoparticles. A RLS method for detecting Lys has been described by Enriquez et al. [35], 11-mercaptoundecanoic acid-capped gold nanoparticles were employed as probes in their research. In addition, gold nanoparticles and antibody conjugated gold nanoparticles have been used to identity oral cancer cells coupled with RLS images [36]. Recently, Chen et al. [37] has proposed a different concept of multi-label molecular imaging that employs resonant light scattering of three-layered gold–dielectric–gold nanoshells to achieve tunable ultrasharp resonance peaks with a 10 nm narrow width. But, Khlebtsov and Khlebtsov [38], think that the tunable ultrasharp resonance peaks cannot be fabricated in reality due to the effects of size-dependent dielectric functions on metal properties for nano-sized particle simulations. These pioneer works have inspired the practical applications of three-layered gold nanoshells in biological system based on RLS.

In this current work, we explore the sensing potential of three-layered gold–dielectric–gold nanoshells based on studying the interdistance changing between RLS peaks. The numerical computations results indicate that the interdistance between the RLS peaks is sensitive to the changes of the surrounding medium refractive index. Sensitivity is higher than when using two-layered gold nanoshell. This indicates that three-layered gold–dielectric–gold nanoshells would be employed as sensors in biosensing based on measuring RLS.

2. Theory and calculation model

We investigate the RLS properties of three-layered gold–dielectric–gold nanoshells and their potential applications in biosensing. Numerical calculations employing the Drude model and the quasi-static theory were carried out for these goals. Geometry of the structure of gold nanoshell in the presence of a gold core is shown in the inset of Fig. 1. The radius of inner gold core is R_1. The middle dielectric layer has a thickness R_2-R_1 and a dielectric constant ε_2. The maximum of shell radius R_3 is 20 nm, which is in the range of the valid nanoparticle radius for the quasi-static theory [39]. The embedding medium has a dielectric constant $\varepsilon_4=n_4^2$. It is important to note that, ε_1 and ε_3 can have real and imaginary frequency-dependent components, which can be written as follows according to Drude model [8,28,40]:

$$\varepsilon_1(\omega)=\varepsilon_3(\omega)=\varepsilon_r+i\varepsilon_i=\varepsilon_b(\omega)-\frac{\omega_p^2/\omega^2}{1+(1/\omega^2\tau^2)}+i\frac{\omega_p^2/\omega^2}{\omega\tau+(1/\omega\tau)} \quad (1)$$

where $\varepsilon_b(\omega)$ is the dielectric function of bulk gold which is due to the inter-band transition and depends on the light frequency. ω_p denotes the plasmon frequency of the bulk metal [8,41], and ω is the frequency of the incident light. The conduction-electron mean free path of bulk gold at room temperature is about 42 nm [42]. In the present work, because the size of the three-layered gold nanoshells (40 nm) is smaller than the bulk electron mean free path, a contribution to the dielectric function that is due to electron surface scattering becomes important. When size-dependent electron scattering becomes important, the size limit relaxation time τ is dependent on the limited mean free path of the

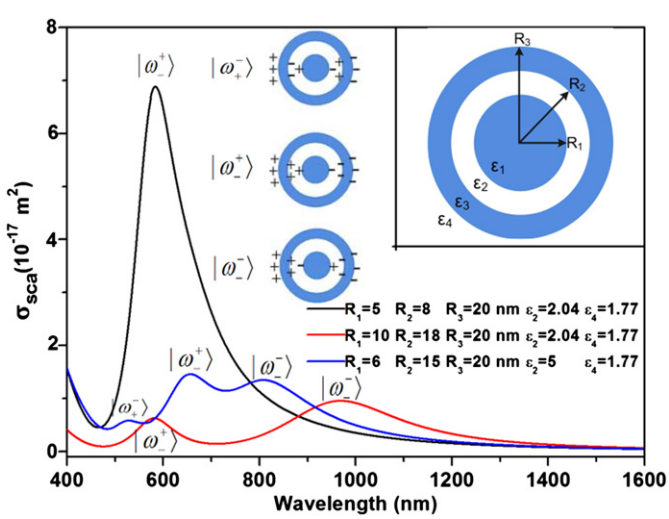

Fig. 1. Light scattering cross section of the three-layered nanoshells with different dimensions. The inset shows the geometry of the structure of the three-layered nanoshells, three kinds of hybridization modes.

electrons, which can be written as [43]

$$\tau = \tau_0 + A\frac{V_F}{L_{\text{eff}}} \tag{2}$$

where τ_0 is the relaxation time in the bulk and V_F is the Fermi velocity. L_{eff} is the effective mean free path. For simple Drude theory and isotropic scattering, $A=1$ [43]. For the inner core, $L_{\text{eff}}=2R_1$, while $L_{\text{eff}}=R_3-R_2$ in the outer shell [12]. However, in present study, we consider the case of $\tau=9.8$ fs for gold nanoshell because of simplifying the calculation. The parameters can be obtained from Refs. [44,45].

The general solution for the potential in each region (the inner core, the middle dielectric layer, the outer layer, and surrounding medium) is given by [43]

$$\Phi_m(r,\theta) = (A_m r + B_m/r^2)\cos\theta \quad (m=1,2,3,4) \tag{3}$$

where A_m and B_m are the constants multiplying the monopole and the dipole terms, respectively. And m is the index of each medium and has a value from 1 to 4. The boundary conditions must be specified so that the potential in each medium can be determined. First, there must be continuity of the tangential component of the electric field:

$$\Phi_m = \Phi_{m+1}\big|_{r=R_1;\, r=R_2;\, r=R_3} \tag{4}$$

Second, there must be continuity of the normal component of the displacement field:

$$\varepsilon_m\left(\frac{\partial\Phi_m}{\partial r}\right) = \varepsilon_{m+1}\left(\frac{\partial\Phi_{m+1}}{\partial r}\right)\Big|_{r=R_1;\, r=R_2;\, r=R_3} \tag{5}$$

In region 1, $B_1=0$; in region 4, far from the shell, we must recover the potential$\Phi_4=-E_0 r\cos\theta$, thus giving $A_4=-E_0$ The boundary conditions (Eqs. (4) and (5)) to Eq. (3) lead to a set of six equations and six unknowns that can be solved to obtain A_1, A_2, B_2, A_3, B_3, and B_4 as follows [28]:

$$A_1 = \frac{27\varepsilon_2\varepsilon_3\varepsilon_4 R_2^3 R_3^3}{a-b-c+d}E_0 \tag{6}$$

$$A_2 = \frac{2\varepsilon_2+\varepsilon_1}{3\varepsilon_2}A_1 \tag{7}$$

$$B_2 = \frac{\varepsilon_2-\varepsilon_1}{3\varepsilon_2}R_1^3 A_1 \tag{8}$$

$$A_3 = \frac{(2\varepsilon_2+\varepsilon_1)(2\varepsilon_3+\varepsilon_2)}{9\varepsilon_2\varepsilon_3}A_1 + \frac{2(\varepsilon_2-\varepsilon_1)(\varepsilon_3-\varepsilon_2)R_1^3}{9\varepsilon_2\varepsilon_3 R_2^3}A_1 \tag{9}$$

$$B_3 = \frac{(2\varepsilon_4+\varepsilon_3)R_3^3}{2(\varepsilon_3-\varepsilon_4)}A_3 + \frac{3\varepsilon_4 R_3^3}{2(\varepsilon_3-\varepsilon_4)}E_0 \tag{10}$$

$$B_4 = A_3 R_3^3 + B_3 + R_3^3 E_0 \tag{11}$$

where

$$a = 2(2\varepsilon_2+\varepsilon_1)(\varepsilon_2-\varepsilon_3)(\varepsilon_4-\varepsilon_3)R_2^6 \tag{12}$$

$$b = 2(\varepsilon_2-\varepsilon_1)(2\varepsilon_2+\varepsilon_3)(\varepsilon_4-\varepsilon_3)R_1^3 R_2^3 \tag{13}$$

$$c = (\varepsilon_1+2\varepsilon_2)(\varepsilon_2+2\varepsilon_3)(\varepsilon_3+2\varepsilon_4)R_2^3 R_3^3 \tag{14}$$

$$d = 2(\varepsilon_2-\varepsilon_1)(\varepsilon_2-\varepsilon_3)(\varepsilon_3+2\varepsilon_4)R_1^3 R_3^3 \tag{15}$$

Then the electric field in each region can be obtained with $E_m=-\nabla\Phi_m(r,\theta)$ [28]:

$$E_1 = A_1(\sin\theta\hat{\theta}-\cos\theta\hat{r}) \tag{16}$$

$$E_2 = A_2(\sin\theta\hat{\theta}-\cos\theta\hat{r}) + \frac{B_2}{r^3}(\sin\theta\hat{\theta}+2\cos\theta\hat{r}) \tag{17}$$

$$E_3 = A_3(\sin\theta\hat{\theta}-\cos\theta\hat{r}) + \frac{B_3}{r^3}(\sin\theta\hat{\theta}+2\cos\theta\hat{r}) \tag{18}$$

$$E_4 = -E_0(\sin\theta\hat{\theta}-\cos\theta\hat{r}) + \frac{B_4}{r^3}(\sin\theta\hat{\theta}+2\cos\theta\hat{r}) \tag{19}$$

When $r=R_3$, $\theta=0$, the electric field in the outer surface of the third gold layer is as follows:

$$E_4 = E_0 + \frac{2}{R_3^3}B_4 \tag{20}$$

The induced field in the region outside the third layer is the same as a dipole with an effective dipole moment. Therefore, outside the third layer the electric field is equivalent to the incident field E_0 plus the field of an electric dipole. From this we can calculate the polarizability of three-layered gold nanoshell as follows:

$$\begin{aligned}\alpha &= 2\pi\varepsilon_0 R_3^3\left(\frac{E_4-E_0}{E_0}\right)\\ &= 2\pi\varepsilon_0 R_3^3\left\{\begin{array}{l}\frac{6\varepsilon_4 R_2^3 R_3^3(2\varepsilon_2+\varepsilon_1)(2\varepsilon_3+\varepsilon_2)}{a-b-c+d} + \frac{12\varepsilon_4 R_1^3 R_3^3(\varepsilon_2-\varepsilon_1)(\varepsilon_3-\varepsilon_2)}{a-b-c+d} + \frac{3\varepsilon_4}{\varepsilon_3-\varepsilon_4} + \\ 2 + \frac{3\varepsilon_4 R_3^3(2\varepsilon_4+\varepsilon_3)}{\varepsilon_3-\varepsilon_4}\left[\frac{R_2^3(2\varepsilon_2+\varepsilon_1)(2\varepsilon_3+\varepsilon_2)}{a-b-c+d} + \frac{2R_1^3(\varepsilon_2-\varepsilon_1)(\varepsilon_3-\varepsilon_2)}{a-b-c+d}\right]\end{array}\right\}\end{aligned} \tag{21}$$

where $\varepsilon_0=8.85\times10^{-12}$ F/m is the permittivity of free space [43]. At last, the scattering cross section could be derived as follows:

$$\sigma_{\text{sca}} = \frac{k^4|\alpha|^2}{6\pi\varepsilon_0^2} \tag{22}$$

where $k=2\pi\sqrt{\varepsilon_4}/\lambda$. After the formulas and parameters were fixed, we write the loop computational procedure and use the well known MATLAB software (Version 7.0) to conduct the simulation. According to different cases, we just need to change the R_1, R_2, ε_2, and ε_4.

3. Results and discussion

3.1. RLS spectra of three-layered gold–dielectric–gold nanoshells

In Fig. 1 the scattering cross section of three-layered gold–dielectric–gold nanoshell as a function of wavelength is shown. Under the different geometrical parameters, the three-layered nanoshells display one, two, and three RLS peaks. Only one light scattering peak appears at 584 nm when $[R_1, R_2, R_3]=[5, 8, 20]$ nm and $[\varepsilon_2, \varepsilon_4]=[2.04, 1.77]$. With $[R_1, R_2, R_3]=[10, 18, 20]$ nm and $[\varepsilon_2, \varepsilon_4]=[2.04, 1.77]$, two light scattering peaks are located at 581 nm and 968 nm. Also, three light scattering peaks take place at 528 nm, 657 nm, and 808 nm respectively with $[R_1, R_2, R_3]=[6, 15, 20]$ nm and $[\varepsilon_2, \varepsilon_4]=[5, 1.77]$.

In general, the resonant light scattering of metal nanostructures originate from their plasmon resonance [46], and this has been verified in gold nanosphere [47], gold nanorod [33], and two-layered gold–dielectric nanoshell [48]. Furthermore, three-layered gold–silica–gold nanoshells also display one, two, and three surface plasmon resonance (SPR) peaks by varying the geometrical parameters [31], arising from the interaction between the gold core and the outer shell [10,12,31]. The interaction leads to a lower energy antisymmetric bonding mode $|\omega_-^-\rangle$, a higher energy symmetric antibonding mode $|\omega_-^+\rangle$, and a nonbonding mode $|\omega_+^-\rangle$[30], illuminated by the theory of plasmon hybridization [49]. The mode $|\omega_-^-\rangle$ and $|\omega_-^+\rangle$ result from the symmetric/antisymmetric coupling between the sphere mode for the inner gold core and the bonding mode for the outer gold nanoshell, which were reported mostly in previous work [10,12,28]. And the mode $|\omega_+^-\rangle$ which can be observed on certain

conditions comes from the symmetric coupling between the sphere mode for the inner gold core and the anti-bonding mode for the outer gold nanoshell [31]. Therefore, the three kinds of RLS modes for three-layered gold–dielectric–gold nanoshells in current research are attributed to the coupling between the sphere mode for the inner gold core and the bonding/anti-bonding mode for the outer gold nanoshell. The short light scattering peak is corresponding to the hybridized non-bonding mode ($|\omega_+^-\rangle$), the middle one corresponds to the hybridized anti-bonding mode ($|\omega_-^+\rangle$), and the long one corresponds to the hybridized bonding mode ($|\omega_-^-\rangle$), as shown in Fig. 1. As the $|\omega_+^-\rangle$ mode does not always appear, in this paper, we just focus on the common type which appears two RLS peaks.

Metal nanotubes which own the similar cross section as the metal nanoshells have attracted the attention of physicists. By employing the plasmon hybridization method, Moradi [50] has investigated plasmonic response of a metallic nanotube and given general expression of the dispersion relation for surface plasmons. The dispersion relation for surface plasmons does not only depend on the angular-momentum, but also the ratio of the inner to outer radius. Wu et al. [51] have calculated the extinction spectra of gold nanotubes by using the vector wave function methods. Effects of geometry, incidence angle, and polarization on the surface plasmon resonance are studied in detail. All of us have used the Drude model and plasmon hybridization method, however, Moradi [50] and Wu et al. [51] solved the Laplace's equation using the Bessel function, we used the general solution according to the Ref. [43]. In addition, the last expressions were different, Moradi [50] gave general expressions of the resonant frequencies of the two plasmon hybridization modes; Wu et al. [51] obtained the extinction efficiency, scattering efficiency, and absorption efficiency in perpendicular and parallel polarization directions; while the expression of scattering cross section was provided in present work. Both Moradi [50] and Wu et al. [51] have observed that the splitting of the plasmons will be large in a nanotube with a thinner shell.

The coated metallic nanowire, consisting of an inner metal core, dielectric spacer layer, and an outer metallic tube [52], has the exact cross section as the three-layered nanoshell in present work. As mentioned in Moradi's work [52], the plasmon hybridization modes of coated metallic nanowire have a behavior similar to that of three-layered nanoshell when the longitudinal wave vector is zero. As the expression of plasmon mode frequencies has been given by Moradi [52], one can obtain the RLS frequency. In fact, the optical property of two-layered gold nanotubes with infinite length has already been studied by using the quasi-static theory [53,54], and the expression of scattering cross section has also been given. In our analysis, if the oversize of the three-layered nanotubes was much smaller than the wavelength of incident light, the quasi-static approximation can be employed in the calculation [3].

3.2. Sensitivity of the interdistance between RLS peaks to the local dielectric environment

Fig. 2 shows the effect of the increased refractive index of the embed medium on the RLS peaks shifting for a given case, where $[R_1, R_2, R_3]=[8, 18, 20]$ nm and $\varepsilon_2=2.04$, and the refractive index of the embed medium n_4 varies from 1.0 to 1.7. As shown in Fig. 2, when n_4 increases, the RLS mode $|\omega_-^-\rangle$ red-shifts, while the RLS mode $|\omega_-^+\rangle$ blue-shifts. As the previous paper reported, increasing the dielectric constant of the embed medium mainly affects the bonding mode for the outer gold nanoshell and hence the plasmon energies of both symmetric and antisymmetric coupling reduce. In other words, the SPR mode $|\omega_-^-\rangle$ and $|\omega_-^+\rangle$ would both red-shift as the refractive index of the surrounding medium

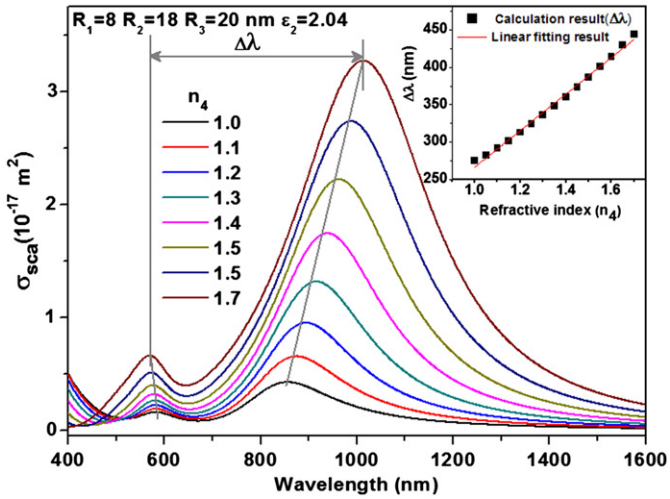

Fig. 2. Light scattering cross section of the three-layered nanoshells with varied refractive index of the embed medium. The inset shows the interdistance between RLS peaks as a function of index of the embed medium.

increases [10,31]. However, for the mode $|\omega_-^+\rangle$, increasing the dielectric constant of the embed medium can reduce the induced electrons on the outer surface of the third gold shell, then the repulsion between the negative charges on the outer surface of the inner core and the outer surface of the third gold shell would decrease, leading to the increase in the restoring force [55]. Thus, the plasmon energies will enhance and the mode $|\omega_-^+\rangle$ blue-shifts. At last, the interdistance between the mode $|\omega_-^+\rangle$ and $|\omega_-^-\rangle$ ($\Delta\lambda$, as shown in Fig. 2) will be more wide as n_4 increases. Furthermore, a good linear relationship between $\Delta\lambda$ and the refractive index is obtained in the range of 1.0 to 1.7, with a sensitivity $\Delta\lambda/\Delta n=243.3$ nm/RIU, as shown in the inset of Fig. 2. This phenomena invited us to systematically investigate the sensing potential of gold–dielectric–gold nanoshells based on the interdistance changing between the two RLS peaks (the mode $|\omega_-^+\rangle$ and $|\omega_-^-\rangle$).

3.3. The effect of geometrical parameters on the shifting of the mode $|\omega_-^+\rangle$

In this paper, the blue-shifting of the mode $|\omega_-^+\rangle$ is the principal cause leading to the $\Delta\lambda$ enhancing as n_4 increases. Under what geometrical conditions the mode $|\omega_-^+\rangle$ would shift to blue when increasing n_4 is urgent to know. Fig. 3 shows the effect of R_1, R_2, and R_3 on the RLS mode $|\omega_-^+\rangle$ shifting when increasing the n_4. Fig. 3a indicates that the mode $|\omega_-^+\rangle$ shifts to blue with R_1 below 10 nm when increasing n_4. As n_4 is more than 1.5, the blue-shifting is more obvious which is suitable for detecting high refractive index solution. The influence of R_2 on the shifting of the mode $|\omega_-^+\rangle$ is shown in Fig. 3b. As n_4 increases, the mode $|\omega_-^+\rangle$ shifts to blue with thicker middle dielectric layer or thinner outer gold shell. Furthermore, with the thinner outer gold shell, the blue-shifting takes place in the range of $n_4=1.0$ to $n_4=2.0$. This suggests that a three-layered gold nanoshell with thin outer gold shell is appropriate for measuring various solutions. In addition, Fig. 3c shows the effect of overall size (R_3) on the shifting of the mode $|\omega_-^+\rangle$. When R_1 and R_2 are fixed, the blue-shifting occurs just as R_3 is slightly more than R_2. Essentially, that is similar to the effect of R_2: a thinner outer gold shell leads to blue-shifting when increasing n_4. However, the influence of R_3 on the mode $|\omega_-^+\rangle$ blue-shifting is less obvious than that of R_2. To sum up, the Fig. 3 indicates that the blue-shifting of the mode

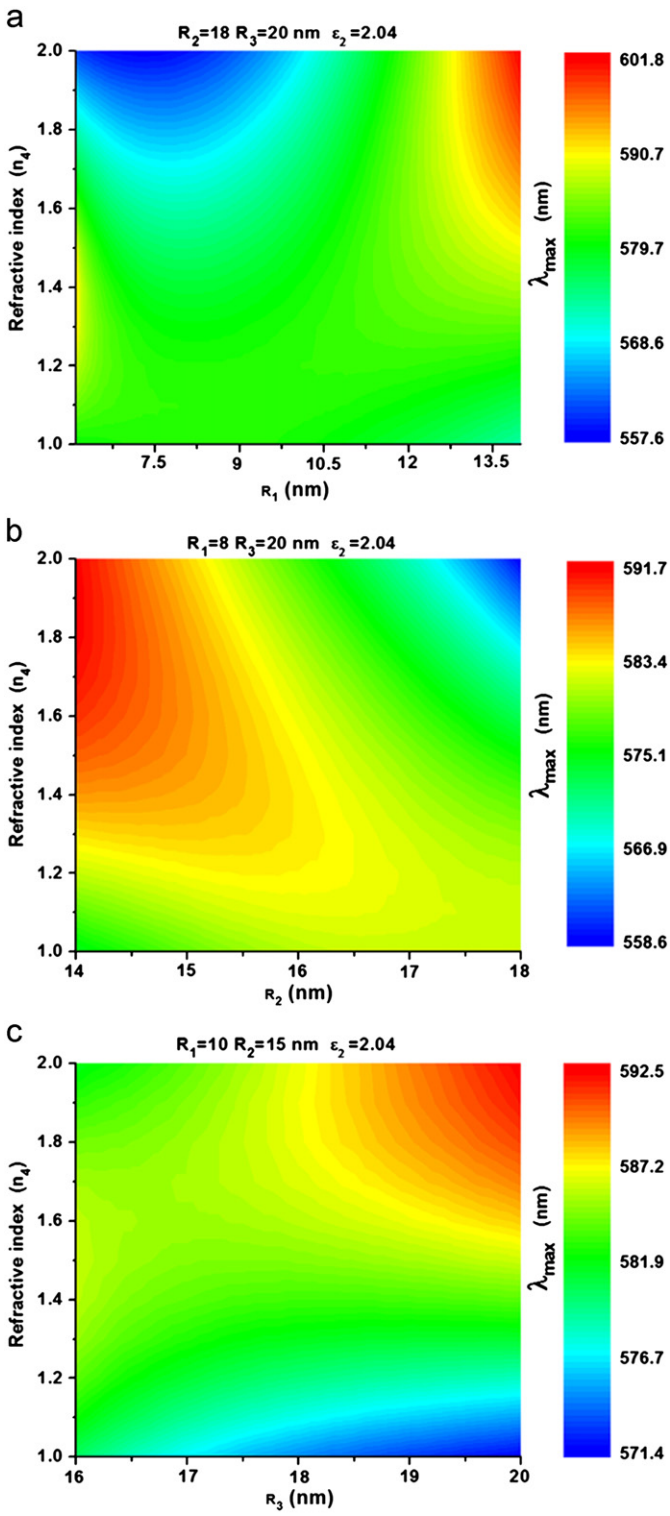

Fig. 3. The position shifting of the mode $|\omega_-^+\rangle$ with different R_1 (a), R_2 (b), and R_3 (c) when increasing the refractive index of physical environment.

$|\omega_-^+\rangle$ is easier to observe in a three-layered gold nanoshell with the thicker dielectric middle layer as the n_4 increases.

3.4. The sensitivity comparison between the three- and two-layered gold nanoshells

As mentioned before, compared with the two-layered gold nanoshell with equal overall size and outer gold shell thickness, the sensitivity of a three-layered gold nanoshell to changes in dielectric environment is lower when measuring the SPR shifting [10]. To figure out whether that is true when detecting the changes of RLS, the sensitivity calculations of three- and two-layered silica–gold nanoshells are carried out. The results are shown in Fig. 4, Fig. 4a represent the three-layered silica–gold nanoshells: interdistance between the mode $|\omega_-^+\rangle$ and $|\omega_-^-\rangle$ as a function of the embed medium refractive index n_4; Fig. 4b represent two-layered silica–gold nanoshells: the mode $|\omega_-^-\rangle$ RLS peak position as a function of the embed medium refractive index n_4. As the outer gold shell thickness is 2 and 3 nm, the sensitivity of the interdistance between the mode $|\omega_-^+\rangle$ and $|\omega_-^-\rangle$ RLS peaks of the three-layered gold nanoshell is below that of the mode $|\omega_-^-\rangle$ RLS peak shifting of the two-layered gold nanoshell. However, the sensitivity of the three-layered gold nanoshell is higher than that of the two-layered gold nanoshell when the outer gold shell thickness decreases to 1 nm. This suggests that the three-layered gold nanoshell with a thin gold shell is superior to the two-layered gold nanoshell in detecting changes in dielectric environment. Fig. 4 also indicates that a thinner outer gold shell is more sensitive to the surrounding refractive index when detecting the RLS behaviors.

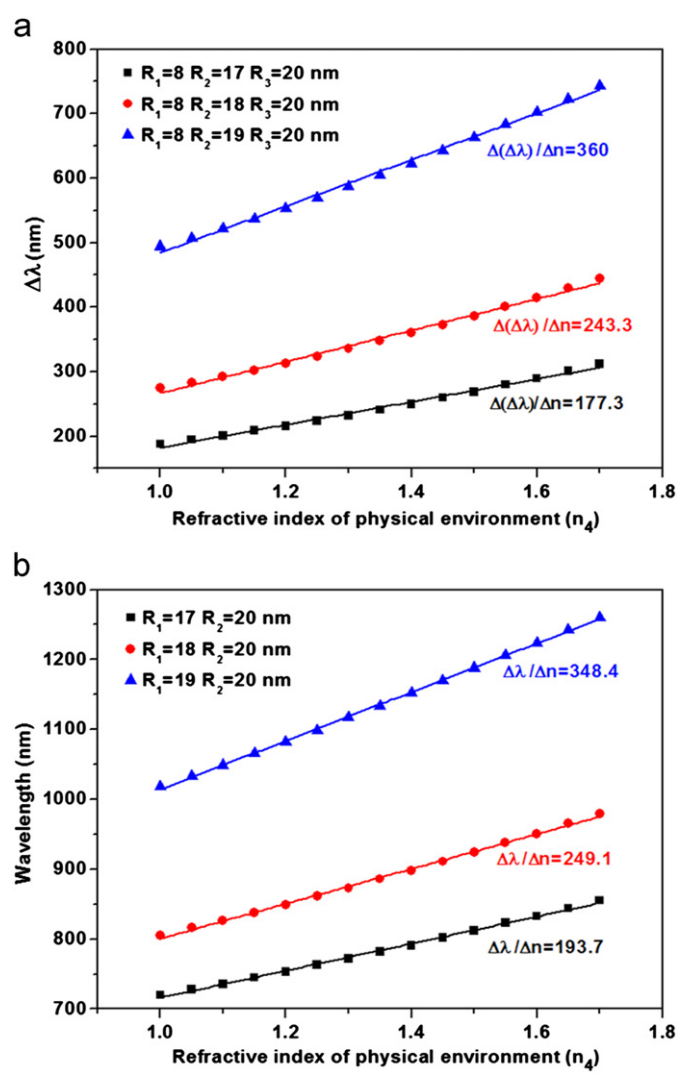

Fig. 4. The sensitivity comparison between the (a) three- and two-layered (b) gold nanoshells with different thickness of the outer gold shell. (For interpretation of the references to color in this figure legend, the reader is referred to the web version of this article.)

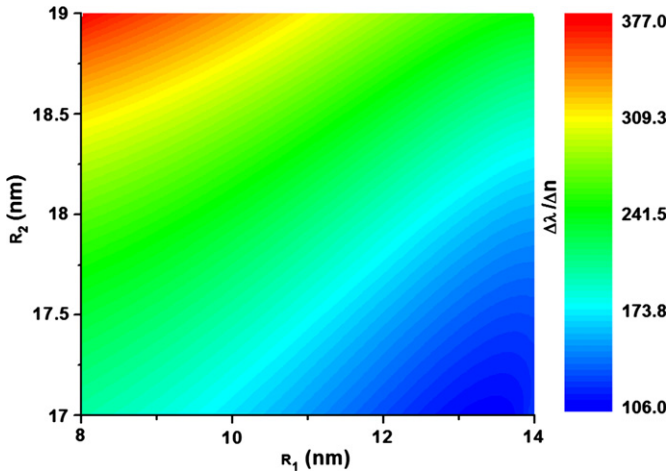

Fig. 5. The sensitivity of the three-layered gold nanoshells with varying the inner core size and the outer shell thickness.

3.5. Sensitivity tunability from geometrical parameters

The effects of geometric parameters on the sensitivity of a three-layered gold nanoshell RLS sensor are shown in Fig. 5. For the three-layered gold nanoshells with oversize $R_3 = 20$ nm, as R_1 increases from 8 to 14 nm and R_2 from 17 to 19 nm, the corresponding sensitivity increases from 106 to 377 nm/RIU. This means that the inner gold core also has the influence on the sensitivity of the three-layered gold nanoshells. Furthermore, the sensitivity is more sensitive to the changes in the thickness of the outer gold shell. Fig. 5 tells us that a three-layered gold nanoshell with a big R_2 and a small R_1 has high sensitivity.

4. Conclusions

In this paper, we have proven that the three-layered gold nanoshells can be used as nanosensors for the local dielectric environment change detection based on interdistance between RLS peaks. The interdistance sensitivity observed is slightly greater than sensitivity achieved using the two-layered gold nanoshells based on RLS peaks shifting. Also, that sensitivity enhances dramatically with increasing R_2 and to a lesser extent with decreasing R_1. The local dielectric environment dependent interdistance changing offers insight to the fabricating nanoshell sensors based on multi RLS peaks for biosensing applications.

Acknowledgments

We acknowledge the financial supports of this research by the National High-tech Research and Development Program (863 Program) of China under Grant no. 2009AA04Z314 and the Fundamental Research Funds for the Central Universities under Grant no. xjj20100049.

References

[1] D.A. Giljohann, D.S. Seferos, W.L. Daniel, M.D. Massich, P.C. Patel, C.A. Mirkin, Angewandte Chemie-International Edition 49 (2010) 3280.
[2] X. Huang, M.A. El-Sayed, Journal of Advanced Research 1 (2010) 13.
[3] U. Kreibig, M. Vollmer, Optical Properties of Metal Clusters, Springer-Verlag, Berlin, Germany, 1995.
[4] P.K. Jain, K.S. Lee, I.H. El-Sayed, M.A. El-Sayed, Journal of Physical Chemistry B 110 (2006) 7238.
[5] K.L. Kelly, E. Coronado, L.L. Zhao, G.C. Schatz, Journal of Physical Chemistry B 107 (2003) 668.
[6] D.J. Wu, X.J. Liu, Applied Physics Letters 97 (2010) 061904.
[7] O. Pena, U. Pal, L. Rodriguez-Fernandez, A. Crespo-Sosa, Journal of the Optical Society of America B: Optical Physics 25 (2008) 1371.
[8] J. Zhu, Applied Physics Letters 92 (2008) 241919.
[9] J. Zhu, J.W. Zhao, J.J. Li, Plasmonics 5 (2010) 311.
[10] Y. Hu, R.C. Fleming, R.A. Drezek, Optics Express 16 (2008) 19579.
[11] Y. Hu, S.J. Noelck, R.A. Drezek, ACS Nano 4 (2010) 1521.
[12] D.J. Wu, X.J. Liu, Applied Physics B 97 (2009) 193.
[13] D.J. Wu, X.J. Liu, Applied Physics Letters 96 (2010) 151912.
[14] D.J. Wu, X.D. Xu, X.J. Liu, Journal of Chemical Physics 129 (2008) 074711.
[15] Y. Zhang, G.T. Fei, L.D. Zhang, Journal of Applied Physics 109 (2011) 054315.
[16] H. Khosravi, N. Daneshfar, A. Bahari, Physics of Plasmas 17 (2010) 0533021.
[17] O. Pena-Rodriguez, U. Pal, Journal of Physical Chemistry C 114 (2010) 4414.
[18] C. Radloff, N.J. Halas, Nano Letters 4 (2004) 1323.
[19] S.J. Oldenburg, R.D. Averitt, S.L. Westcott, N.J. Halas, Chemical Physics Letters 288 (1998) 243.
[20] S.J. Oldenburg, J.B. Jackson, S.L. Westcott, N.J. Halas, Applied Physics Letters 75 (1999) 2897.
[21] Y. Wang, X. Xie, X. Wang, G. Ku, K.L. Gill, D.P. O'Neal, G. Stoica, L.V. Wang, Nano Letters 4 (2004) 1689.
[22] R. Shukla, V. Bansal, M. Chaudhary, A. Basu, R.R. Bhonde, M. Sastry, Langmuir 21 (2005) 10644.
[23] S. Kalele, S.W. Gosavi, J. Urban, S.K. Kulkarni, Current Science 91 (2006) 1038.
[24] C. Loo, A. Lowery, N. Halas, J. West, R. Drezek, Nano Letters 5 (2005) 709.
[25] L.R. Hirsch, J.B. Jackson, A. Lee, N.J. Halas, J.L. West, Analytical Chemistry 75 (2003) 2377.
[26] F. Tam, C. Moran, N.J. Halas, Journal of Physical Chemistry B 108 (2004) 17290.
[27] X.H. Xia, Y. Liu, V. Backman, G.A. Ameer, Nanotechnology 17 (2006) 5435.
[28] J. Zhu, Y.J. Ren, S.M. Zhao, J.W. Zhao, Materials Chemistry and Physics 133 (2012) 1060.
[29] K. Hasegawa, C. Rohde, M. Deutsch, Optics Letters 31 (2006) 1136.
[30] R. Bardhan, S. Mukherjee, N.A. Mirin, S.D. Levit, P. Nordlander, N.J. Halas, Journal of Physical Chemistry C 114 (2009) 7378.
[31] J. Zhu, J.J. Li, J.W. Zhao, Plasmonics 6 (2011) 527.
[32] D.R.H. Craigf., F. Bohren, Absorption and Scattering of Light by Small Particles, Wiley &Sons, Inc, New York, 1983.
[33] J. Zhu, L.Q. Huang, J.W. Zhao, Y.C. Wang, Y.R. Zhao, L.M. Hao, Y.M. Lu, Materials Science and Engineering: B 121 (2005) 199.
[34] L. Shang, H.J. Chen, L. Deng, S.J. Dong, Biosensors and Bioelectronics 23 (2008) 1180.
[35] A.C. Enriquez, I.A.R. Espejel, E.A. Garcia, M.E. Diaz-Garcia, Analytical and Bioanalytical Chemistry 391 (2008) 807.
[36] I.H. El-Sayed, X.H. Huang, M.A. El-Sayed, Nano Letters 5 (2005) 829.
[37] K. Chen, Y. Liu, G. Ameer, V. Backman, Journal of Biomedical Optics 10 (2005) 024005.
[38] B. Khlebtsov, N. Khlebtsov, Journal of Biomedical Optics 11 (2006) 044002.
[39] J. Zhu, X. Liu, Chemical Physics 323 (2006) 446.
[40] J.A.A.J. Perenboom, P. Wyder, F. Meier, Physics Reports 78 (1981) 173.
[41] E. Prodan, A. Lee, P. Nordlander, Chemical Physics Letters 360 (2002) 325.
[42] N.W. Ashcroft, N.D. Mermin, Holt, Rinehart and Winston, New York, 1976.
[43] R.D. Averitt, S.L. Westcott, N.J. Halas, Journal of the Optical Society of America B: Optical Physics 16 (1999) 1824.
[44] D. Canchal-Arias, P. Dawson, Surface Science 577 (2005) 95.
[45] P.B. Johnson, R.W. Christy, Physical Review B 6 (1972) 4370.
[46] J. Zhu, Y.C. Wang, L.Q. Huang, Y.M. Lu, Physics Letters A 323 (2004) 455.
[47] J. Zhu, J.C. Wang, Plasma Science and Technology 5 (2003) 1835.
[48] G.J. Weng, J.J. Li, J. Zhu, J.W. Zhao, Colloids and Surfaces, A 369 (2010) 253.
[49] E. Prodan, C. Radloff, N.J. Halas, P. Nordlander, Science 302 (2003) 419.
[50] A. Moradi, Journal of Physics and Chemistry Of Solids 69 (2008) 2936.
[51] D. Wu, X. Liu, B. Li, Journal of Applied Physics 109 (2011) 083540.
[52] A. Moradi, Journal of the Optical Society of America B, Optical Physics 29 (2012) 625.
[53] J. Zhu, J.J. Li, J.W. Zhao, Journal of Computational and Theoretical Nanoscience 7 (2010) 2291.
[54] J. Zhu, Materials Science and Engineering A 454 (2007) 685.
[55] S.N. Yan, Y.C. Wang, T.D. Wen, J. Zhu, Physica E 33 (2006) 139.